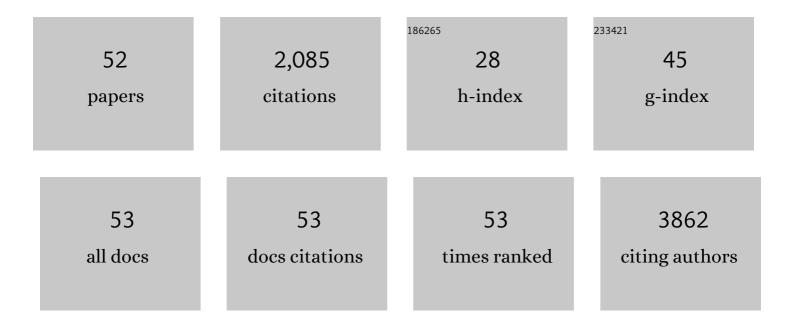
Xuefeng Song

List of Publications by Year in descending order

Source: https://exaly.com/author-pdf/9216961/publications.pdf Version: 2024-02-01



#	Article	IF	CITATIONS
1	Coating of Phosphide Catalysts on p-Silicon by a Necking Strategy for Improved Photoelectrochemical Characteristics in Alkaline Media. ACS Applied Materials & Interfaces, 2021, 13, 20185-20193.	8.0	10
2	Metal organic framework derived Ni/CeO2 catalyst with highly dispersed ultra-fine Ni nanoparticles: Impregnation synthesis and the application in CO2 methanation. Ceramics International, 2021, 47, 12366-12374.	4.8	33
3	Enhancing the Long-Term Photoelectrochemical Performance of TiO ₂ /Si Photocathodes by Coating of Ti-Doped Mesoporous Hematite. ACS Applied Energy Materials, 2021, 4, 7882-7890.	5.1	4
4	Visible lightâ€activated degradation of microcystin‣R by ultrathin gâ€C ₃ N ₄ nanosheetsâ€based heterojunction photocatalyst. Journal of the American Ceramic Society, 2020, 103, 1281-1292.	3.8	13
5	Electrode material of core-shell hybrid MoS2@C/CNTs with carbon intercalated few-layer MoS2 nanosheets. Materials Today Energy, 2020, 16, 100379.	4.7	21
6	Interfacial electrochemical investigation of 3D space-confined MnFe2O4 for high-performance ionic liquid-based supercapacitors. Electrochimica Acta, 2020, 331, 135386.	5.2	22
7	Interface guide: In-situ integrating MoS2 nanosheets into highly ordered polypyrrole film for high performance flexible supercapacitor electrodes. Composites Science and Technology, 2020, 197, 108263.	7.8	12
8	Engineering defectâ€enabled 3D porous MoS ₂ /C architectures for high performance lithiumâ€ion batteries. Journal of the American Ceramic Society, 2020, 103, 4453-4462.	3.8	20
9	Confinement Effect of Mesopores: In Situ Synthesis of Cationic Tungsten-Vacancies for a Highly Ordered Mesoporous Tungsten Phosphide Electrocatalyst. ACS Applied Materials & Interfaces, 2020, 12, 22741-22750.	8.0	34
10	Hybrid Nanostructured Ni(OH)2/NiO for High-Capacity Lithium-Ion Battery Anodes. Journal of Electrochemical Energy Conversion and Storage, 2020, 17, .	2.1	4
11	A robust quasiâ€superhydrophobic ceria coating prepared using airâ€plasma spraying. Journal of the American Ceramic Society, 2019, 102, 1386-1393.	3.8	19
12	Visible Light-Activated Self-Recovery Hydrophobic CeO ₂ /Black TiO ₂ Coating Prepared Using Air Plasma Spraying. ACS Applied Materials & Interfaces, 2019, 11, 37209-37215.	8.0	13
13	Highly coke resistant Mg–Ni/Al ₂ O ₃ catalyst prepared <i>via</i> a novel magnesiothermic reduction for methane reforming catalysis with CO ₂ : the unique role of Al–Ni intermetallics. Nanoscale, 2019, 11, 1262-1272.	5.6	29
14	Bioinspired pomegranate-like microflowers confining core-shell binary Ni _x S _y nanobeads for efficient supercapacitors exhibiting a durable lifespan exceeding 100 000 cycles. Journal of Materials Chemistry A, 2019, 7, 3432-3442.	10.3	19
15	Engineering the volumetric effect of Polypyrrole for auto-deformable supercapacitor. Chemical Engineering Journal, 2019, 374, 59-67.	12.7	33
16	Foamy Photocathode with Cu ₂ O Nanowire Arrays Decorated with Cu ₂ O and Carbon Layer for Photoelectrochemical Hydrogen Evolution. Journal of the Electrochemical Society, 2019, 166, H452-H458.	2.9	5
17	Generation of Monolayer MoS ₂ with 1T Phase by Spatialâ€Confinementâ€Induced Ultrathin PPy Anchoring for Highâ€Performance Supercapacitor. Advanced Materials Interfaces, 2019, 6, 1900162.	3.7	33
18	Self‣upporting Electrode of High Conductive PEDOT:PSS/CNTs Coaxial Nanocables Wrapped by MnO ₂ Nanosheets. ChemistrySelect, 2019, 4, 2009-2017.	1.5	4

XUEFENG SONG

#	Article	IF	CITATIONS
19	A comprehensive study on surface integrity of nickel-based superalloy Inconel 718 under robotic belt grinding. Materials and Manufacturing Processes, 2019, 34, 61-69.	4.7	35
20	Enhanced photoelectrochemical performance and stability of Si nanowire photocathode with deposition of hematite and carbon. Applied Surface Science, 2019, 471, 528-536.	6.1	13
21	A robust hierarchical microcapsule for efficient supercapacitors exhibiting an ultrahigh current density of 300 A g ^{â''1} . Journal of Materials Chemistry A, 2018, 6, 5724-5732.	10.3	15
22	An Investigation of Surface Corrosion Behavior of Inconel 718 after Robotic Belt Grinding. Materials, 2018, 11, 2440.	2.9	14
23	Hollow hierarchical Ni/MgO-SiO2 catalyst with high activity, thermal stability and coking resistance for catalytic dry reforming of methane. International Journal of Hydrogen Energy, 2018, 43, 11056-11068.	7.1	44
24	A novel sound-based belt condition monitoring method for robotic grinding using optimally pruned extreme learning machine. Journal of Materials Processing Technology, 2018, 260, 9-19.	6.3	55
25	Sustainable Energy System Utilizing Highâ€Voltageâ€Stable and Energyâ€dense Supercapacitors Based on Porous Fe ₂ O ₃ @Graphene Electrode in Ionic Liquid Electrolyte. Energy Technology, 2018, 6, 2399-2407.	3.8	7
26	Integrated Sustainable Wind Power Harvesting and Ultrahigh Energy Density Wireâ€Shaped Supercapacitors Based on Vertically Oriented Nanosheetâ€Arrayâ€Coated Carbon Fibers. Advanced Sustainable Systems, 2017, 1, 1700044.	5.3	11
27	Recoverable Wire-Shaped Supercapacitors with Ultrahigh Volumetric Energy Density for Multifunctional Portable and Wearable Electronics. ACS Applied Materials & Interfaces, 2017, 9, 17051-17059.	8.0	31
28	Enhanced photoelectrochemical performance of planar p-Silicon by APCVD deposition of surface mesoporous hematite coating. Applied Catalysis B: Environmental, 2017, 200, 372-377.	20.2	12
29	High rate lithium-ion batteries from hybrid hollow spheres with a few-layered MoS ₂ -entrapped carbon sheath synthesized by a space-confined reaction. Journal of Materials Chemistry A, 2016, 4, 10425-10434.	10.3	63
30	Highly Conductive Mo ₂ C Nanofibers Encapsulated in Ultrathin MnO ₂ Nanosheets as a Self-Supported Electrode for High-Performance Capacitive Energy Storage. ACS Applied Materials & Interfaces, 2016, 8, 32460-32467.	8.0	49
31	Active Fe ₂ O ₃ nanoparticles encapsulated in porous g-C ₃ N ₄ /graphene sandwich-type nanosheets as a superior anode for high-performance lithium-ion batteries. Journal of Materials Chemistry A, 2016, 4, 10666-10672.	10.3	94
32	Size-engineerable NiS 2 hollow spheres photo co-catalysts from supermolecular precursor for H 2 production from water splitting. Chemical Engineering Journal, 2016, 290, 74-81.	12.7	31
33	A Silicon/Double-Shelled Carbon Yolk-Like Nanostructure as High-Performance Anode Materials for Lithium-Ion Battery. Journal of the Electrochemical Society, 2015, 162, A1530-A1536.	2.9	42
34	A MnOOH/nitrogen-doped graphene hybrid nanowires sandwich film for flexible all-solid-state supercapacitors. Journal of Materials Chemistry A, 2015, 3, 6136-6145.	10.3	49
35	Heating-Rate-Induced Porous α-Fe ₂ O ₃ with Controllable Pore Size and Crystallinity Grown on Graphene for Supercapacitors. ACS Applied Materials & Interfaces, 2015, 7, 75-79.	8.0	100
36	Covalently Coupled Ultrafine H-TiO ₂ Nanocrystals/Nitrogen-Doped Graphene Hybrid Materials for High-Performance Supercapacitor. ACS Applied Materials & Interfaces, 2015, 7, 17884-17892.	8.0	119

XUEFENG SONG

#	Article	IF	CITATIONS
37	Phyllosilicate evolved hierarchical Ni- and Cu–Ni/SiO2 nanocomposites for methane dry reforming catalysis. Applied Catalysis A: General, 2015, 503, 94-102.	4.3	78
38	Photoelectrochemical Hydrogen Production of TiO ₂ Passivated Pt/Si-Nanowire Composite Photocathode. ACS Applied Materials & Interfaces, 2015, 7, 18560-18565.	8.0	65
39	Template-assisted synthesis of multi-shelled carbon hollow spheres with an ultralarge pore volume as anode materials in Li-ion batteries. RSC Advances, 2015, 5, 3657-3664.	3.6	32
40	Sol–gel nanocasting synthesis of kesterite Cu ₂ ZnSnS ₄ nanorods. RSC Advances, 2015, 5, 1220-1226.	3.6	28
41	Micro―and Nanostructures of Photoelectrodes for Solarâ€Driven Water Splitting. Advanced Materials, 2015, 27, 562-568.	21.0	50
42	Controlled synthesis of yolk–mesoporous shell Si@SiO ₂ nanohybrid designed for high performance Li ion battery. RSC Advances, 2014, 4, 20814-20820.	3.6	32
43	Capacitors: Selfâ€Assembled αâ€Fe ₂ O ₃ Mesocrystals/Graphene Nanohybrid for Enhanced Electrochemical Capacitors (Small 11/2014). Small, 2014, 10, 2308-2308.	10.0	1
44	Ultrathin Ti-doped hematite photoanode byÂpyrolysis of ferrocene. International Journal of Hydrogen Energy, 2014, 39, 14596-14603.	7.1	21
45	Cu ₂ ZnSnS ₄ thin films: spin coating synthesis and photoelectrochemistry. RSC Advances, 2014, 4, 21318-21324.	3.6	49
46	Facile synthesis of hollow hierarchical Ni/γ-Al ₂ O ₃ nanocomposites for methane dry reforming catalysis. RSC Advances, 2014, 4, 51184-51193.	3.6	50
47	Selfâ€Assembled αâ€Fe ₂ O ₃ Mesocrystals/Graphene Nanohybrid for Enhanced Electrochemical Capacitors. Small, 2014, 10, 2270-2279.	10.0	177
48	Surfactant-free hydrothermal synthesis of Cu ₂ ZnSnS ₄ (CZTS) nanocrystals with photocatalytic properties. RSC Advances, 2014, 4, 27805-27810.	3.6	72
49	Cu–Ni@SiO2 alloy nanocomposites for methane dry reforming catalysis. RSC Advances, 2013, 3, 23976.	3.6	59
50	Crumpled nitrogen-doped graphene–ultrafine Mn3O4 nanohybrids and their application in supercapacitors. Journal of Materials Chemistry A, 2013, 1, 14162.	10.3	72
51	Facile Synthesis of Nitrogen-Doped Graphene–Ultrathin MnO ₂ Sheet Composites and Their Electrochemical Performances. ACS Applied Materials & Interfaces, 2013, 5, 3317-3322.	8.0	173
52	A hierarchical hybrid design for high performance tin based Li-ion battery anodes. Nanotechnology, 2013, 24, 205401.	2.6	13